Time-Domain BEM for Dynamic Crack Problems in Thin Piezoelectric Structures

Hongjun Zhong[1], Jun Lei[1,*], Chuanzeng Zhang[2]

[1] Department of Engineering Mechanics, Beijing University of Technology, 100124, China
[2] Department of Civil Engineering, University of Siegen, D-57076 Siegen, Germany
* Corresponding author: leijun@bjut.edu.cn

Abstract A 2-D time-domain boundary element method (BEM) is developed to study the static and dynamic fracture problems in thin piezoelectric structures under electromechanical loadings. The traditional displacement boundary integral equations (BIEs) are applied on the external boundary and the hypersingular traction BIEs are applied on the crack faces. The present time-domain BEM uses a quadrature formula for the temporal discretization to approximate the convolution integrals and a collocation method for the spatial discretization. Quadratic quarter-point elements are implemented at the crack tip. The strongly singular and hypersingular integrals are evaluated by a regularization technique based on a suitable variable change. The nearly singular integrals arisen in thin structures are dealt with by two ways. The first one is based on a nonlinear coordinate transformation method for curve-quadratic elements. The second method is on an analytical integration method for straight quadratic elements to avoid the nearly singularity. A displacement extrapolation technique is used to determine the dynamic intensity factors (DIFs) including the dynamic stress intensity factors (DSIFs) and dynamic electrical displacement intensity factor (DEDIF). Some examples are presented to verify the effectiveness and stability of present BEM in thin piezoelectric structures.

Keywords thin piezoelectric structure, time-domain boundary element method, nearly singular integration, dynamic intensity factors

1. Introduction

With intrinsic electro-mechanical coupling characteristics, piezoelectric materials are widely used in smart structures. For typical engineering piezoelectric materials like PZT and PVDF, it's difficult to be applied to the complicated shape structures. Therefore, painting technology is developed, which forms piezoelectric coatings on the structures to produce electro-mechanical coupling function. But cracks may occur in the coating or between the coating and the matrix during preparation or under complex electro-mechanical loadings. So it's significant to study the fracture problems in the thin piezoelectric structure.

For general dynamic crack problems in piezoelectric materials, numerical methods are more feasible due to the mathematical complexity of the initial boundary value problems. Particularly, Boundary Element Method (BEM) has certain advantages in fracture analysis. In 2008, time-domain BEM for transient dynamic crack analysis of linear piezoelectric solids was implemented by García-Sánchez et al. [1], who used the Lubich convolution quadrature formula for the temporal discretization and a collocation method for the spatial discretization. However, its extension to dynamic cracks in thin piezoelectric structures is not straight-forward, since the corresponding dynamic Green's functions have quite complicated mathematical structures, which generate nearly singularity during integration when the field point is very close to the source point. In 2002, Liu and Fan [2] successfully applied the BEM in the static analysis of thin piezoelectric solids. The nearly singular integrals were solved by an analytical method. But they didn't take cracks into consideration.

To apply the time-domain BEM to the crack analysis of thin piezoelectric structures, two methods are developed to deal with the nearly singular integrals. The first one is based on a nonlinear coordinate transformation method for curve-quadratic elements. The second method is on an analytical integration method for straight quadratic elements. Numerical results are presented to verify the accuracy of the present integral equations and the time-domain BEM.

2. Time-domain BIEs for Piezoelectric Materials

2.1. Piezoelectric Equations

Consider a 2D homogeneous, linear cracked piezoelectric solid occupying domain Ω with boundary Γ. To describe the electric-elastic fields, the 'extended' variables u_J, f_J, σ_{iJ}, ε_{Ji} are defined:

$$u_J = \begin{cases} u_j \\ \phi \end{cases}, \quad f_J = \begin{cases} f_j & J = j = 1,2 \\ -q & J = 3 \end{cases}, \quad \sigma_{iJ} = \begin{cases} \sigma_{ij} \\ D_i \end{cases}, \quad \varepsilon_{Ji} = \begin{cases} \varepsilon_{ji} & J = j = 1,2 \\ E_i & J = 3 \end{cases}, \tag{1}$$

which combine the elastic variables involving the displacement u_j, body force f_j, stress σ_{ij}, strain ε_{ij}, and the electric ones including electric potential ϕ, charge q, electrical displacement D_j, field E_j. Without body forces and electrical charge, the governing equations and the constitutive equations under quasi-electrostatic assumption are given by

$$\sigma_{iJ,i} = \rho \delta^*_{JK} \ddot{u}_K, \quad \sigma_{iJ} = C_{iJKl} \varepsilon_{Kl}, \tag{2}$$

where ρ is the mass density, "," designates spatial derivative, while "$\cdot$" denotes temporal derivative. The capital index is from 1 to 3 while lower case letter index takes 1 or 2. The extended Kronecker delta δ^*_{JK} is defined by

$$\delta^*_{JK} = \begin{cases} \delta_{JK} & J,K = 1,2 \\ 0 & \text{otherwise} \end{cases}. \tag{3}$$

Material constants C_{iJKl} are as follows,

$$C_{iJKl} = \begin{cases} c_{ijkl}, & J = j = 1,2; \quad K = k = 1,2 \\ e_{jil}, & K = 3; \quad J = j = 1,2 \\ e_{kli}, & J = 3; \quad K = k = 1,2 \\ -\kappa_{il}, & J = K = 3 \end{cases}. \tag{4}$$

in which c_{ijkl}, e_{ijk} and κ_{ik} are the elasticity constants, piezoelectric constants and dielectric constants, respectively. The extended strain and displacement relations are given by

$$\varepsilon_{ij} = \left(u_{i,j} + u_{j,i}\right)/2, \quad E_i = -\varphi_{,i}. \tag{5}$$

2.2. Time-domain Boundary Integral Equations

On the boundary Γ, the displacement and traction BIEs are

$$c_{IJ}(\boldsymbol{x}_0) u_J(\boldsymbol{x}_0, t) = \int_\Gamma \left(u^{\mathrm{G}}_{IJ} * p_J - p^{\mathrm{G}}_{IJ} * u_J \right) \mathrm{d}\Gamma + \int_{\Gamma^+_C} p^{\mathrm{G}}_{IJ} * \Delta u_J \mathrm{d}\Gamma, \quad \boldsymbol{x}_0 \in \Gamma, \tag{6}$$

$$p_J(\boldsymbol{x}_0, t) = \int_\Gamma \left(d^{\mathrm{G}}_{IJ} * p_J - s^{\mathrm{G}}_{IJ} * u_J \right) \mathrm{d}\Gamma + \int_{\Gamma^+_C} s^{\mathrm{G}}_{IJ} * \Delta u_J \mathrm{d}\Gamma, \quad \boldsymbol{x}_0 \in \Gamma^+_C, \tag{7}$$

where $c_{IJ}(\boldsymbol{x})$ are free term constants, "$*$" denotes Riemann convolution, Δu_J are the extended crack-opening-displacements, u^G_{IJ} and p^G_{IJ} are 2D time-domain dynamic displacement and the

traction fundamental solutions. d_{IJ}^{G} and s_{IJ}^{G} are fundamental solutions of higher order. These fundamental solutions have been derived by Wang and Zhang [3].

2.3. Laplace-domain dynamic fundamental solutions

The traction fundamental solutions p_{IJ}^{G} and d_{IJ}^{G} have a strong singularity of Cauchy type, while the higher-order traction fundamental solution s_{IJ}^{G} has a hypersingularity. To deal with the singularity, it is advantageous to split the fundamental solutions into a singular static part and a regular dynamic part. The singular static parts are given by

$$p_{IJ}^{\mathrm{G(S)}}\left(\boldsymbol{x}_0,\boldsymbol{x}\right)=\frac{1}{\pi}\mathrm{Re}\left[\sum_{M=1}^{3}L_{JM}Q_{MI}\,\frac{\mu_M n_1(\boldsymbol{x})-n_2(\boldsymbol{x})}{z_M-z_M^0}\right], \tag{8}$$

$$d_{IJ}^{\mathrm{G(S)}}\left(\boldsymbol{x}_0,\boldsymbol{x}\right)=-\frac{1}{\pi}\mathrm{Re}\left[\sum_{M=1}^{3}L_{JM}Q_{MI}\,\frac{\mu_M n_1(\boldsymbol{x}_0)-n_2(\boldsymbol{x}_0)}{z_M-z_M^0}\right], \tag{9}$$

$$s_{IJ}^{\mathrm{G(S)}}\left(\boldsymbol{x}_0,\boldsymbol{x}\right)=\frac{1}{\pi}\mathrm{Re}\left[\sum_{M=1}^{3}T_{IJ}^{M}\,\frac{\mu_M n_1(\boldsymbol{x})-n_2(\boldsymbol{x})}{(z_M-z_M^0)^2}\right], \tag{10}$$

where

$$z_M=x+\mu_M y,\ \ z_M^0=x_0+\mu_M y_0,\ \ M=1,2,3. \tag{11}$$

$\boldsymbol{x}_0(x_0,y_0)$ is the source point while $\boldsymbol{x}(x,y)$ the observation point. L_{JM}, Q_{MI}, T_{IJ}^{M} and μ_M are determined by the anisotropic material constants [3].

2.4. Time-stepping scheme

To approximate the Riemann convolution integrals in BIEs, Lubich quadrature formula is used [1]

$$f\left(t\right)=g\left(t\right)*h\left(t\right)\cong\sum_{j=0}^{n}\omega_{n-j}\left(\Delta t\right)h\left(j\Delta t\right), \tag{12}$$

where time t is divided into N equal time-steps, and the weights $\omega_{n-j}\left(\Delta t\right)$ are determined by

$$\omega_{n-j}\left(\Delta t\right)=\frac{r^{-(n-j)}}{N}\sum_{m=0}^{N-1}\hat{g}\left[\delta\left(\zeta_m\right)/\Delta t\right]\mathrm{e}^{-2\pi i\cdot(n-j)m/N}, \tag{13}$$

in which $\hat{g}\left(\cdot\right)$ stands for the Laplace-transformation of the function $g(t)$. After the temporal and spatial discretization, a system of linear equations for the discrete boundary quantities can be obtained. Leaving all the unknown boundary quantities on the left-hand side, an explicit time-stepping scheme

$$\boldsymbol{x}_k^n=\left(\mathbf{A}_{kl}^0\right)^{-1}\cdot\left(\boldsymbol{y}_l^n-\sum_{j=1}^{n-1}\mathbf{A}_{kl}^{n-j}\cdot\boldsymbol{x}_l^j\right), \tag{14}$$

can be obtained for computing the unknown boundary quantities at the n-th time-step.

3. Computation of singular integrals

When a collocation point is on one element Γ_e, the BIEs possess strongly singular and hypersingular integrals. After discretization, the singular integrals correspond to the following integrals,

$$I_M=\int_{\Gamma_e}\frac{\mu_M n_1(\boldsymbol{x})-n_2(\boldsymbol{x})}{z_M-z_M^0}\phi_q d\Gamma,\ \ I_M'=\int_{\Gamma_e}\frac{\mu_M n_1(\boldsymbol{x})-n_2(\boldsymbol{x})}{(z_M-z_M^0)^2}\phi_q d\Gamma \tag{15}$$

where ϕ_q (q=1,2,3) is the quadratic shape function and $\boldsymbol{n}(\boldsymbol{x})$ donates the outward unit normal

vector to the boundary. A complex variable is introduced as

$$\chi_M = z_M - z_M^0 = x - x_0 + \mu_M (y - y_0) . \tag{16}$$

With this transformation,

$$I_M = \int_{\Gamma_e} \frac{1}{\chi_M} \phi_q d\chi_M , \quad I'_M = \int_{\Gamma_e} \frac{1}{\chi_M^2} \phi_q d\chi_M . \tag{17}$$

ϕ_q can be considered as a function of χ_M, and its first Taylor series at $\chi_M = 0$ is

$$\phi_q(\chi_M) = \phi_q(\chi_M = 0) + \mathrm{O}(\chi_M) = \phi_{q0} + \mathrm{O}(\chi_M) . \tag{18}$$

With the substitution of Eq. (18) into I_M,

$$I_M = \int_{\Gamma_e} \frac{1}{\chi_M} (\phi_q - \phi_{q0}) d\chi_M + \phi_{q0} \int_{\Gamma_e} \frac{1}{\chi_M} d\chi_M . \tag{19}$$

The first part in Eq. (19) can be calculated by Gaussian quadrature formula. The second integral is strongly singular but can be evaluated analytically as

$$\int_{\Gamma_e} \frac{1}{\chi_M} d\chi_M = \log(\chi_M)|_{\Gamma_e} . \tag{20}$$

For I'_M, the Taylor-series is expanded to two terms. Then, the integral can be transformed to

$$I'_M = \int_{\Gamma_e} \frac{\phi_q - (\phi_{q0} + \phi'_{q0} \cdot \chi_M)}{\chi_M^2} d\chi_M + \phi_{q0} \int_{\Gamma_e} \frac{1}{\chi_M^2} d\chi_M + \phi'_{q0} \int_{\Gamma_e} \frac{1}{\chi_M} d\chi_M . \tag{21}$$

The first integral can be computed by Gaussian integral quadrature. The second and third integral can be evaluated analytically as

$$\int_{\Gamma_e} \frac{1}{\chi_M^2} d\chi_M = -\frac{1}{\chi_M}\bigg|_{\Gamma_e} , \quad \int_{\Gamma_e} \frac{1}{\chi_M} d\chi_M = \log(\chi_M)|_{\Gamma_e} . \tag{22}$$

4. Computation of nearly singular integrals

When the collocation point is very close to the integration point in thin piezoelectric structures, nearly singular integrals appear. To deal with this problem, two methods are developed for curve quadratic elements and straight quadratic element. On the analogy of the solution to the singular problems in section 3, the nearly singular integrals can be classified into three kinds

$$J_M = \int_{\Gamma_e} \frac{\mu_M n_1(\boldsymbol{x}) - n_2(\boldsymbol{x})}{z_M - z_M^0} \phi_q d\Gamma , J'_M = \int_{\Gamma_e} \frac{\mu_M n_1(\boldsymbol{x}) - n_2(\boldsymbol{x})}{(z_M - z_M^0)^2} \phi_q d\Gamma , J''_M = \int_{\Gamma_e} \frac{\mu_M n_1(\boldsymbol{x}_0) - n_2(\boldsymbol{x}_0)}{z_M - z_M^0} \phi_q d\Gamma . \tag{23}$$

4.1. Curve quadratic element

For isoparametric quadratic element, similar method as the singular integrals can be applied. Local coordinate system of $\xi[-1,1]$ is introduced. When collocation point $\boldsymbol{x}_0$ is very close to Γ_e, the nearest point on Γ_e to $\boldsymbol{x}_0$ is assumed to be $\boldsymbol{Q}(x', y')$ which has the local coordinate ξ', so

$$z'_M = x' + \mu_M y' . \tag{24}$$

Let $\chi_M = z_M - z'_M$, $\chi_M^0 = z'_M - z_M^0$, so J_M can be transformed into

$$J_M = \int_{\Gamma_e} \frac{1}{\chi_M + \chi_M^0} \phi_q d\chi_M . \tag{25}$$

With the substitution of Taylor expansion of ϕ_q, J_M can be separated into two parts as follows

$$J_M = \int_{\Gamma_e} \frac{\phi_q - \phi_{q0}}{\chi_M + \chi_M^0} d\chi_M + \phi_{q0} \int_{\Gamma_e} \frac{1}{\chi_M + \chi_M^0} d\chi_M . \tag{26}$$

The second integral can be calculated analytically as

$$\int_{\Gamma_e} \frac{1}{\chi_M + \chi_M^0} d\chi_M = \log(\chi_M + \chi_M^0)|_{\Gamma_e} . \tag{27}$$

For the first integral in Eq.(26), with the substitution of local coordinate ξ, the detailed formulation for q=1 is

$$\int_{\Gamma_e} \frac{\phi_1 - \phi_{10}}{\chi_M + \chi_M^0} d\chi_M = \int_{\Gamma_e} \frac{[\mu_M(c\xi + d) + (a\xi + b)][(\xi - \xi')^2 + (\xi - \xi')(2\xi' - \xi_3)]}{(\xi_1 - \xi_3)\xi_1[a_M(\xi - \xi')^2 + b_M(\xi - \xi') + c_M]} d\xi , \tag{28}$$

where

$$a_M = \frac{a + \mu_M c}{2}, b_M = 2a_M\xi' + (b + \mu_M d), c_M = a_M\xi'^2 + (b + \mu_M d)\xi' + (x_2 - x_0) + \mu_M(y_2 - y_0) . \tag{29}$$

ξ_i (i=1,2,3) are the local coordinates of the collocation points on the element. With a linear transformation $\zeta = \xi - \xi'$, Eq. (28) can be transformed into

$$\int_{\Gamma_e} \frac{\phi_1 - \phi_{10}}{\chi_M + \chi_M^0} d\chi_M = \int_{\Gamma_e} \frac{[\mu_M(c\zeta + c\xi' + d) + (a\zeta + a\xi' + b)][\zeta^2 + \zeta(2\xi' - \xi_3)]}{(\xi_1 - \xi_3)\xi_1(a_M\zeta^2 + b_M\zeta + c_M)} d\zeta . \tag{30}$$

Then nonlinear transformation $\zeta = \varsigma^m$ proposed by Luo et al. [4] can be added to Eq. (30), so that it can be calculated using the standard Gaussian quadrature formula.

For J'_M, second Taylor series are essential, and the equation can be separated into three parts as

$$J'_M = \int_{\Gamma_e} \frac{\phi_q - (\phi_{q0} + \phi'_{q0}\chi_M)}{(\chi_M + \chi_M^0)^2} d\chi_M + \int_{\Gamma_e} \frac{\phi_{q0} - \phi'_{q0}\chi_M^0}{(\chi_M + \chi_M^0)^2} d\chi_M + \int_{\Gamma_e} \frac{\phi'_{q0}}{\chi_M + \chi_M^0} d\chi_M . \tag{31}$$

The third part can be evaluated as in Eq. (27), and the second part can also be evaluated by

$$\int_{\Gamma_e} \frac{1}{(\chi_M + \chi_M^0)^2} d\chi_M = -\frac{1}{\chi_M + \chi_M^0}\bigg|_{\Gamma_e} . \tag{32}$$

With linear transformation, the first part when $q = 1$ can be transformed into

$$\int_{\Gamma_e} \frac{\phi_1 - (\phi_{10} + \phi'_{10}\chi_M)}{(\chi_M + \chi_M^0)^2} d\chi_M = \int_{\Gamma_e} \frac{[\mu_M(c\xi + d) + (a\xi + b)][1 - (2\xi' - \xi_3)a_M / b_M]\zeta^2}{(\xi_1 - \xi_3)\xi_1(a_M\zeta^2 + b_M\zeta + c_M)^2} d\zeta , \tag{33}$$

nonlinear transformation can also be applied.

For the cases $q = 2$ and $q = 3$, the integrals J_M and J'_M can be evaluated in the same way as the case $q = 1$.

For J''_M, with the substitution of

$$\psi_q = \frac{\mu_M n_1(\mathbf{x}_0) - n_2(\mathbf{x}_0)}{\mu_M n_1(\mathbf{x}) - n_2(\mathbf{x})}\phi_q , \tag{34}$$

it can be changed into

$$J''_M = \int_{\Gamma_e} \frac{1}{\chi_M + \chi_M^0}\psi_q d\chi_M , \tag{35}$$

which has a similar form to J_M. So it can be evaluated with the advantage of the first Taylor-expansion series of ψ_q. The formulation is so complicated that it isn't listed here.

4.2. Straight element

For isoparametric quadratic element, the denominators of the nearly singular integrals possess a relative high order of ξ, which brings difficulty for the integration. So the non-isoparametric quadratic straight line element is introduced. The boundary quantities are described by the same shape functions as the isoparametric quadratic element, while the geometry quantities x and y can be described as

$$x = \frac{x_3 - x_1}{2}\xi + \frac{x_1 + x_3}{2}, \quad y = \frac{y_3 - y_1}{2}\xi + \frac{y_1 + y_3}{2}, \tag{36}$$

in which (x_1, y_1) and (x_3, y_3) are respectively the start and end point of the element. With the above expressions, $z_M - z_M^0$ can be represented by a linear function of ξ,

$$z_M - z_M^0 = (a + \mu_M c)\xi + (b + \mu_M d) - (x_0 + \mu_M y_0), \tag{37}$$

where $a = \frac{x_3 - x_1}{2}$, $b = \frac{x_1 + x_3}{2}$, $c = \frac{y_3 - y_1}{2}$, $d = \frac{y_1 + y_3}{2}$. So ξ gains the following expression,

$$\xi = \frac{z_M - z_M^0 - [b - x_0 + \mu_M (d - y_0)]}{a + \mu_M c}. \tag{38}$$

Nearly singular integrals can be expressed as

$$L_M = \int_{\Gamma_e} \frac{\phi_q}{z_M - z_M^0} dz_M, \quad L'_M = \int_{\Gamma_e} \frac{\phi_q}{(z_M - z_M^0)^2} dz_M. \tag{39}$$

$$L''_M = \frac{[\mu_M n_1(\boldsymbol{x}_0) - n_2(\boldsymbol{x}_0)]\sqrt{a^2 + c^2}}{A_M} \int_{\Gamma_e} \frac{\phi_q}{z_M - z_M^0} dz_M. \tag{40}$$

As the difference between L''_M and L_M is just a coefficient, only Eq. (39) should be evaluated.

Let $q = 1$, with the substitution of Eq. (38) into ϕ_1, the shape functions can be expressed as

$$\phi_1 = \frac{(z_M - z_M^0)^2 - [2B_M + (\xi_2 + \xi_3)A_M](z_M - z_M^0) + (B_M + \xi_2 A_M)(B_M + \xi_3 A_M)}{A_M^2 (\xi_1 - \xi_2)(\xi_1 - \xi_3)}, \tag{41}$$

where $A_M = a + \mu_M c$, $B_M = b - x_0 + \mu_M (d - y_0)$. Therefore L_M can be separated into three parts as follows,

$$\begin{aligned} \int_{\Gamma_e} \frac{\phi_1}{z_M - z_M^0} dz_M = & \frac{1}{(\xi_1 - \xi_2)(\xi_1 - \xi_3)A_M^2} \int_{\Gamma_e} (z_M - z_M^0) dz_M - \frac{2B_M + (\xi_2 + \xi_3)A_M}{(\xi_1 - \xi_2)(\xi_1 - \xi_3)A_M^2} \int_{\Gamma_e} dz_M \\ & + \frac{(B_M + \xi_2 A_M)(B_M + \xi_3 A_M)}{(\xi_1 - \xi_2)(\xi_1 - \xi_3)A_M^2} \int_{\Gamma_e} \frac{1}{z_M - z_M^0} dz_M \end{aligned}. \tag{42}$$

The three integrals can be evaluated analytically,

$$\int_{\Gamma_e} (z_M - z_M^0) dz_M = \left. \frac{(z_M - z_M^0)^2}{2} \right|_{\Gamma_e}, \tag{43}$$

$$\int_{\Gamma_e} dz_M = z_M \big|_{\Gamma_e}, \quad \int_{\Gamma_e} \frac{1}{z_M - z_M^0} dz_M = \log(z_M - z_M^0) \big|_{\Gamma_e} \tag{44}$$

With similarity of the expressions, the integrals can be evaluated in the same way when $q = 2, 3$.

Similarly, L'_M can also be divided into three parts. Two of them can be integrated by Eq. (44), the other one can be evaluated as follows,

$$\int_{\Gamma_e} \frac{1}{(z_M - z_M^0)^2} dz_M = -\frac{1}{z_M - z_M^0}\Big|_{\Gamma_e} . \tag{45}$$

With straight line element applied, the nearly singular integrals can be integrated analytically, and the separated parts have simple expressions.

5. Numerical examples

5.1. A central crack in finite plate

For the first example, a central crack of length 2*a* in a homogeneous and linear piezoelectric plate is considered to verify the correctness of the two methods. As shown in Fig. 1, the plate with width 2L × height 2H is under a pure uniform mechanical tensile loading of $\sigma_0 = 1\text{Mpa}$.

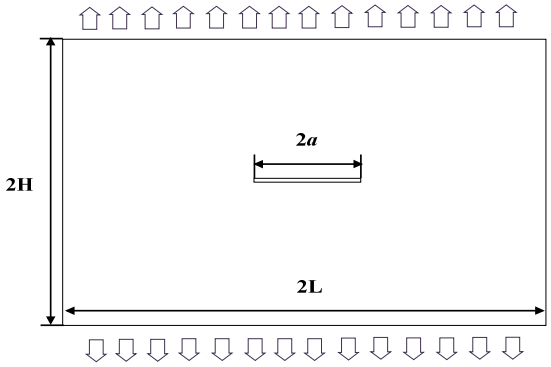

Figure 1. A central crack in a piezoelectric plate

Normalized stress intensity factor $K_I/(\sigma_0\sqrt{\pi a})$ is presented versus L/*a* of the finite plate, the results have been plotted and compared with the corresponding FEM results presented by Cao and Kuang [5] to test the accuracy of the present integration methods. Different heights are considered with H/*a*=0.368, 0.568, 0.968 and 4.618. The two methods coincide well with each other, and they also match well with the FEM results. It should be pointed out that the FEM results are obtained for the condition that the thickness *b* of the plate is 0.01*a*. It can be found from Fig.2 that the values of SIF are approaching to the stable values when the ratio of L/*a* is larger than 2.0, which means these values reach the case of a central crack in the corresponding strips with the height 2H.

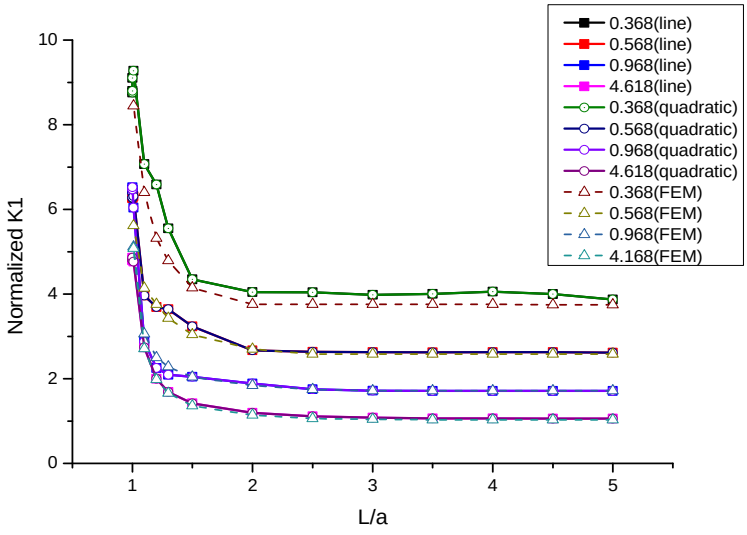

Figure 2. Normalized stress intensity factors for different dimensions

5.2. A central crack in thin piezoelectric structure

When H decreases to a very small value, the plate becomes piezoelectric film. Since the film is thin, the crack length is set to be relatively small. Let L/a=25, 50, normalized stress intensity factor $K_I/(\sigma_0\sqrt{\pi a})$ is presented versus H/*a* which is changing from 1 to 1×10^{-6}. When the ratio is as small as 10^{-6}, it is sufficient for modeling many thin piezoelectric films as used in smart materials and micro-electro-mechanical systems.

With the decrease of H, the stress intensity factor keep increasing when the strip is relatively thick, namely H/*a* is higher than 0.01. But in the interval [0, 0.01], the SIFs become stable. Since the crack is small, the value of $K_I/(\sigma_0\sqrt{\pi a})$ is not so high. For the straight line element method, the stress intensity factors at H/*a*=1×10^{-6} jump slightly.

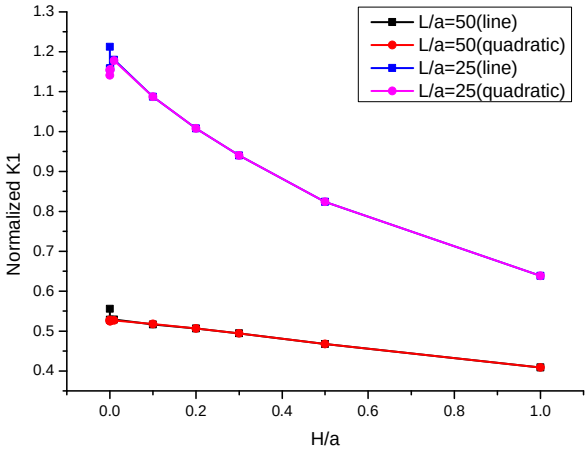

Figure 3. Normalized stress intensity factors versus H/*a*

Dynamic intensity factors are also taken into consideration. For H/*a*=0.1, L/*a*=25, Fig. 3 shows the normalized dynamic intensity factors versus dimensionless time tc_L/H, where

$$c_L=\sqrt{(C_{22}+e_{22}^2/\varepsilon_{22})/\rho}\,. \tag{46}$$

The methods of line element and quadratic element are both used and the results coincide with each other very well.

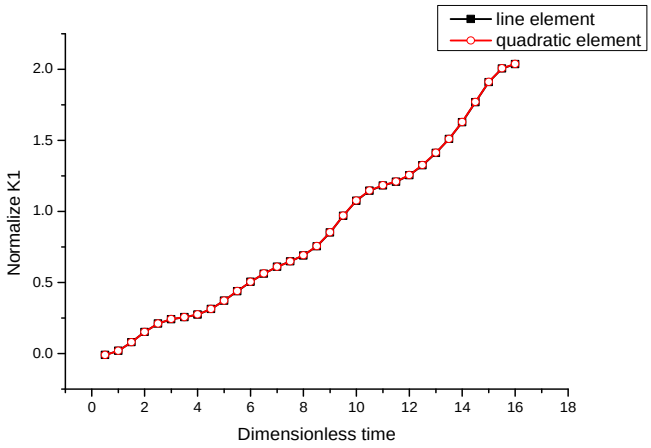

Figure 4. Normalized dynamic stress intensity factors versus dimensionless time

6. Conclusions

Transient dynamic crack problems in piezoelectric thin structures are considered. Two methods are presented to deal with the nearly singular problems in the Laplace domain fundamental solutions. The first method for quadratic element is semi-analytical and the second method for straight line element is analytical. Static stress intensity factor of a piezoelectric plate is obtained for different structural dimensions. The results have been compared with FEM results and the agreement verifies the accuracy of the present methods. Then cracks in thin structures are considered, normalized intensity factors of both static and dynamic cases are obtained. The results indicate that the two methods function well when the ratio of the film thickness to the crack length is as small as 10^{-6} which is sufficient for modeling many thin piezoelectric films and coatings.

Acknowledgements

This work is supported by the Natural Science Foundation of China under Grant No. 11002006 and the German Research Foundation (DFG) under the project number ZH 15/6-1 and ZH 15/6-3, which are gratefully acknowledged.

References

[1] F. García-Sánchez, C.H. Zhang, A. Sáez, 2-D transient dynamic analysis of cracked piezoelectric solids by a time-domain BEM. Comput. Methods Appl. Mech. Engrg., 197 (2008) 3108–3121.

[2] Y.J. Liu, H. Fan, Analysis of thin piezoelectric solids by the boundary element method. Comput. Methods Appl. Mech. Engrg., 191 (2002) 2297–2315.

[3] C.Y. Wang, C.H. Zhang, 3-D and 2-D dynamic Green's functions and time-domain BIEs for piezoelectric solid. Engineering Analysis with Boundary Elements, 29 (2005) 454–465.

[4] J.F. Luo, Y.J. Liu, E.J. Berger, Analysis of two-dimensional thin structures (from micro- to nano-scales) using the boundary element method. Computational Mechanics, 22 (1998) 404–412.

[5] Z.J. Cao, Z.B. Kuang, A finite element modeling for directly determining intensity factors of piezoelectric materials with cracks. Int J Fract, 149 (2008) 67–85.